Talanta 82 (2010) 1403–1411

Contents lists available at ScienceDirect

Talanta

journal homepage: www.elsevier.com/locate/talanta

# Modeling the analytical response of optical fiber sensors for aromatic compounds determination

Lurdes I.B. Silva [a,*], Miguel Freitas [b], Teresa A.P. Rocha-Santos [a,b], A.C. Duarte [a]

[a] CESAM & Department of Chemistry, University of Aveiro, Campus universitário de Santiago, 3810-193 Aveiro, Portugal
[b] ISEIT/Viseu – Instituto Piaget, Estrada do Alto do Gaio, Galifonge, 3515-776 Lordosa, Viseu, Portugal

ARTICLE INFO

*Article history:*
Received 12 April 2010
Received in revised form 29 June 2010
Accepted 3 July 2010
Available online 31 July 2010

*Keywords:*
Analytical response modeling
Optical fiber sensors
SDS calibration model

ABSTRACT

In recent years, there has been an increasing interest in the application of optical fiber sensors for in situ monitoring of chemical pollutants, including volatile organic compounds, regarding air quality assurance. In order to enhance the usefulness and applicability of this methodology to environmental analysis, a proper study of the analytical signal and an adequate calibration model are required. This contribution is focused on the model for optical fiber sensors calibration, discussing some problems associated with the estimates of the figures of merit of these analytical systems. We also suggest and discuss a calibration model based on a cumulative symmetric double sigmoidal (SDS) function, as a suitable and general alternative to the more limited and classical linear calibration model.



## 1. Introduction

Over the last several years, the development of chemical sensors and biosensors based on optical fiber (OF) technology has been investigated resulting in highly suitable devices for various analytical applications. The use of OF devices offers some particular advantages (i.e., immunity to electromagnetic interference and electrically passive operation, small size, robustness, versatility, high sensitivity and accuracy, portability, remote and real-time sensing) over conventional electronic sensing techniques, which make them very suitable for bio/chemical and environmental monitoring purposes [1–22].

The successful application of these sensors depend on the accurate processing of the analytical signal of the OF device, which can often be very complex and extensively characterized by non-linearities. In fact, the general major disadvantage of the OF sensors is either its logistic [23,24] or sigmoidal [6–10] response which produces a limited useable linear region [6–15]. Several signal processing methods [25–29], consisting of development/use of techniques for enhancing the analytical measurements, and calibration models [30–34], have been applied for modeling the analytical response of OF analyzers and to overcoming the analytical problems associated to its complexity. Linear models are often preferred, because they are simple to apply and amenable to straightforward physico-chemical interpretation. For instance, Chang et al. [35] established a linear relationship between alpha-fetoprotein in human serum (in log scale) and fluorescent fiber-optic signal. Such a logit linearization allowed to evaluate and compare localized surface plasmon coupled fluorescence fiber-optic biosensor with the conventional ELISA and radioimmunoassay (RIA). The same approach was been implemented by Jin et al. [36], Kocincova et al. [37] and Solís et al. [38] for dealing with the non-linear behavior of the OF chemical sensors. Capitán-Vallvey et al. [39] have developed a method for linearization of the analytical response of optical devices, based on the logarithmic transformation of the sigmoidal calibration curve with the consequent expansion of the range of linear calibration.

Although in previous studies by Silva et al. [6–10], the OF devices sensitized with polymeric siloxane films also showed a sigmoid like response during volatile organic compounds (VOCs) monitoring, the use of linear models based only on the central part of the sigmoid curve proved to be practical and satisfactory for OF sensors calibration. However, such a truncation of the entire calibration range highlighted the loss of full analytical information besides providing estimates of the figures of merit, such as the detection limit and sensitivity, with no practical significance. This work aims at the determination of the calibration model that fits best the experimental data obtained in the case of the response observed for OF sensors and also to assess the practical meaning of choosing the appropriate model, in the estimative of the various parameters that characterize the quality of the analytical process. In order to attain such a goal a cumulative symmetric double sigmoidal (SDS) model is applied to optical fiber sensors, as an alternative for both classical sigmoidal and linear calibration models.

* Corresponding author. Tel.: +351 232 910 100; fax: +351 232 910 183.
*E-mail address:* lisilva@ua.pt (L.I.B. Silva).

0039-9140/$ – see front matter © 2010 Elsevier B.V. All rights reserved.
doi:10.1016/j.talanta.2010.07.009

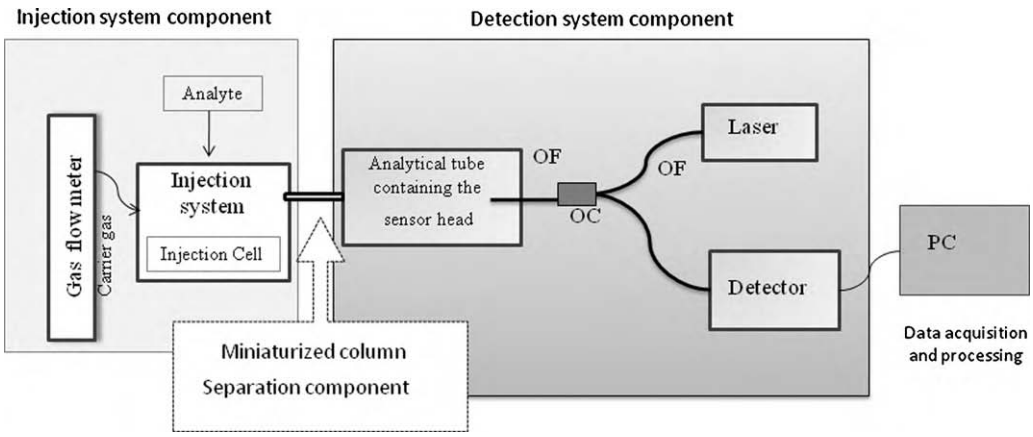


**Fig. 1.** Experimental set-up of the OF sensors for aromatic compounds determination: OC—optical coupler (Y 50:50), OF—optical fiber, PC—laptop for data acquisition and processing.

## 2. Calibration experiments of the OF sensors

The modeling of the analytical response of the OF sensors was performed, taking into account the sensor behavior for aromatic compounds reported elsewhere [6–10]. Fig. 1 shows a generic diagram of the design of the OF devices under study. In general terms, the OF devices are constituted by an injection system component and a detection component, which is constituted by an optical source (laser diode) to generate the interrogating signal, a photodiode to measure the intensity modulated signal and an OF with the top end surface coated with a nanometric film of siloxane polymers (sensor head). These OF analyzers can also incorporate a miniaturized column which promotes the separation of organic compounds mixtures. The sensing principle underlying these sensor devices is based on the changes of the reflected optical power, taken as the analytical signal, when organic vapors are present in the analytical tube, containing the sensitized OF (i.e., the sensor head). The interaction of organic vapors with the polymeric film (sensitive surface) promotes reversible changes in its optical properties (refractive index), leading to a detectable modulation of the light power guided through the OF. The intensity of the modulated reflected signal (analytical signal, in dB) is proportional to the amount of analyte present at the analytical tube and depends on the sensitive film of siloxane polymer, waveguide and analyte properties, as well on the interactions between analyte and polymeric sensitive film.

Fig. 2a shows the sensor response for different amounts of benzene, toluene and xylene (*p*-xylene) in a range between 0.02 and 0.10 μg, performing five repeated evaluations for each amount tested. The OF device shows different analytical responses and calibration sensitivity (inferred from the slope of the calibration curves) for the different aromatic compounds under study: benzene (751 dB $\mu g^{-1}$), toluene (891 dB $\mu g^{-1}$) and *p*-xylene (941 dB $\mu g^{-1}$). The analytical sensitivity increases in the same order as the increase of the analyte boiling temperature in °C (80.1 for benzene <110.6 for toluene <138.4 for *p*-xylene) and the decrease of vapor pressure in mm Hg at 25 °C (95.2 for benzene >28.4 for toluene >8.8 for *p*-xylene). This sensor behavior, that is, the different response and sensitivity based on the different analyte properties (i.e. boiling temperature and vapor pressure) has been also reported elsewhere [6,9].

From the results obtained during the analysis of different amounts of aromatic compounds, it could be verified that for very low quantities of analyte the system remains essentially dormant, producing variations of no practical interest to Analytical Chemistry purposes. Once reached a certain minimum value of the concentration or quantity of analyte, the sensor response increases at an almost constant rate with increasing analyte quantities. Finally, at high values of analyte the sensor response reaches a plateau in terms of its detection capability and from which it also reaches an area of no further practical interest to Analytical Chemistry. In summary, it could be verified that the OF sensor provides an area of rapid change in the analytical signal, centered between two areas of slightly pronounced change of the analytical signal (see Fig. 2a). The shape of the above described response profile may derive from a combination of several factors of sensing and instrumental nature, such as optical source and photodetector properties, and sensitive layer characteristics (chemical and optical properties of the sensing material, thickness, and surface morphology).

This type of response profile was also verified for different designs of OF devices, such as enzymatic based biosensors [4].

Fig. 2b shows the OF device response profile for different amounts of toluene (used as proxy for volatile organic compounds) evaluated, ranging from 0.03 to 0.09 μg. Fig. 2c shows the low variability of the OF sensor response in the determination of 0.04 μg of toluene in five consecutive experiments. The signal corresponding to 0.04 μg of toluene shows a variation of 1.8% measured as the coefficient of variation. This kind of devices shows typically a high stability during different weeks of continuous operation. Fig. 2d shows, as an example, the sensor response (mean and standard deviation of five repeated evaluations) for 0.06 μg of toluene during four weeks; the ANOVA applied to the obtained results showed that there is not a statistically significant difference between weeks ($p = 0.448$).

## 3. Linear range of the analytical response of the OF sensors

Fig. 3a shows the linear range of the sensor response for toluene determination (used as proxy for volatile organic compounds), which will be studied according to the classical approach of linear regression by the least squares method. The analysis of the residuals constitutes a very important tool for assessing how suitable the linear calibration is, in our case. A calibration curve properly adjusted should provide errors with an uniform distribution, of zero mean and constant variance (homogeneity) [40,41]. Fig. 3b shows the distribution of the residuals obtained for the linear model used for calibration and its inspection allows concluding about the suitability of the applied linear model, as the residuals vary in a range of about ±2% and in only two cases, in a total of 25, reaches values higher than 2%, that is, −3% in one case and +5% in another.

The adjustment of the calibration curve using all the experimental points (in a range between 0.04 and 0.08 μg), based on the linear calibration model was performed using TableCurve2D [42] and is shown in Table 1. The parameters and

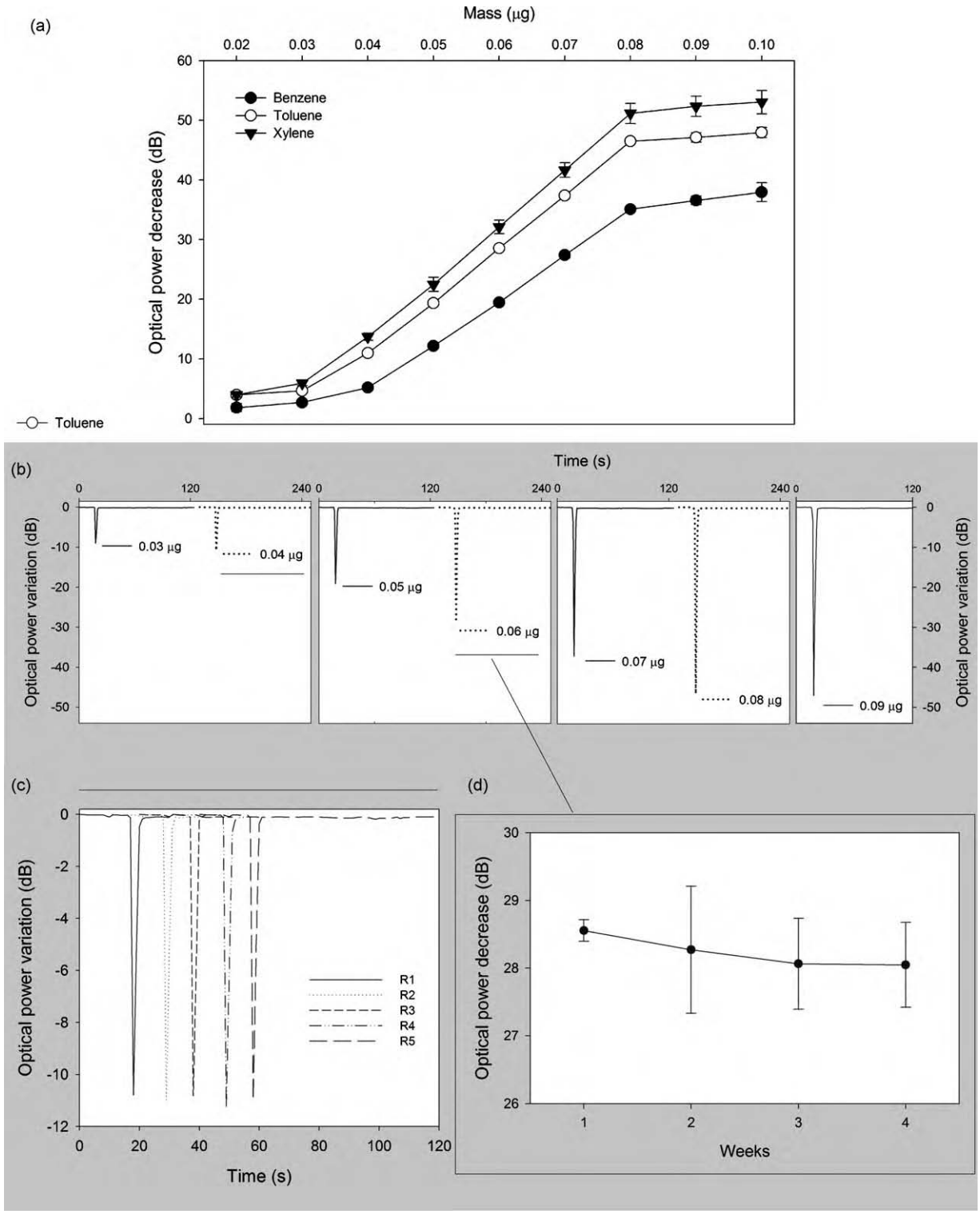


**Fig. 2.** Response of the OF sensor for different amounts of benzene, toluene and xylene injected in a range between 0.02 μg and 0.10 μg (a); response of the OF sensor for different amounts of toluene (b); sensor response obtained during the determination of toluene (0.04 μg) in five sequential experiments, R1–R5 (c); sensor response (mean and standard deviation of five repeated evaluations) for 0.06 μg of toluene during four weeks (d).

the ANOVA results obtained for the linear calibration model, allow concluding that the linear model provides an appropriated adjustment to the set of experimental data evaluated. That is, the relationship between the dependent variable (optical power decrease) and the independent variable (analyte mass) can adequately be depicted through a straight line. This conclusion relies mainly on the high values of the determination coefficient ($R^2$) and *F*-test with their level of significance $p < 0.0001$.

## 4. Determination of the calibration model of the OF sensors

The use of only the linear range of the OF sensor response does not describe either completely or correctly the analytical

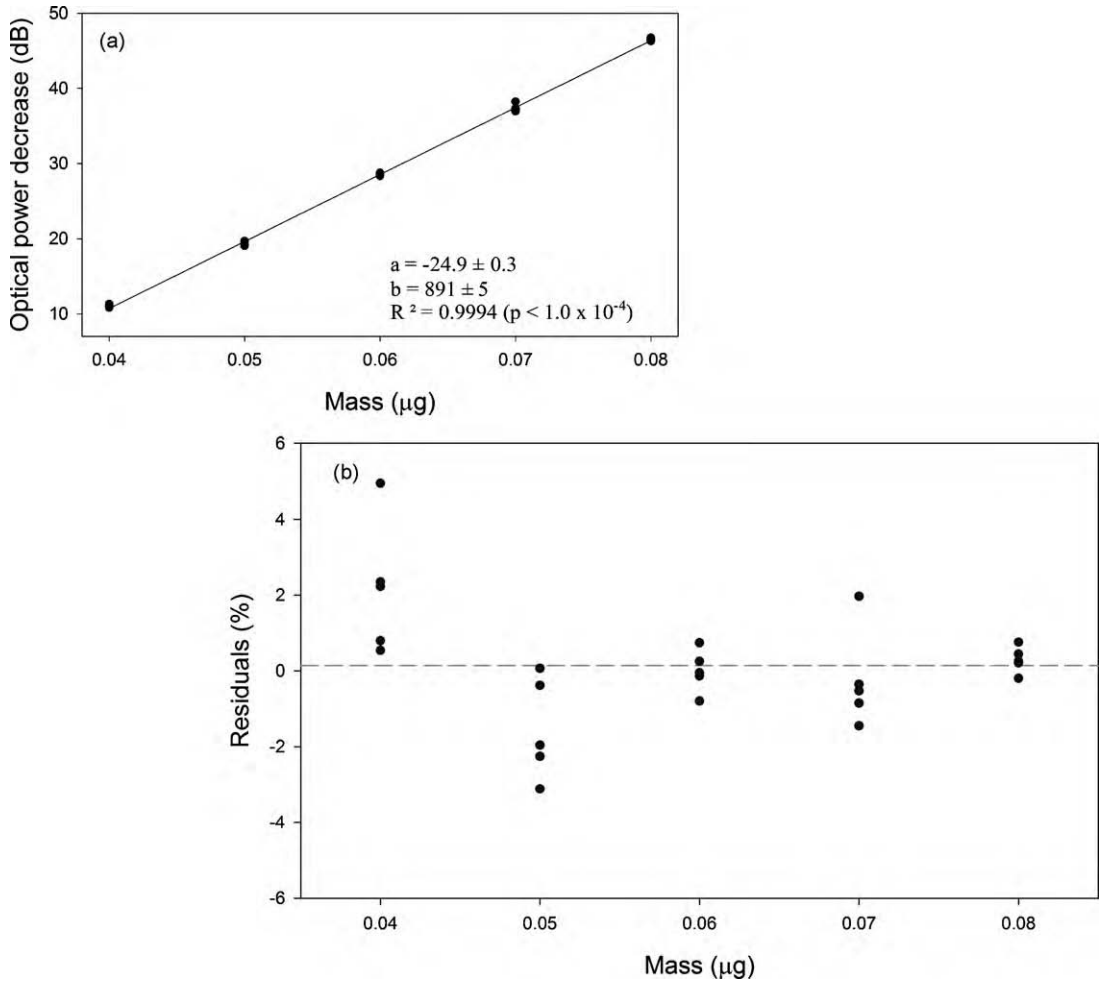


**Fig. 3.** Linear response of the OF sensor for amounts of toluene in a range between 0.04 and 0.08 μg (a); residuals obtained for the linear model used for calibration (b).

performance of the sensor system in the full range of working concentrations or amounts of analyte. A calibration model valid for the whole range of the analytical response of the OF sensor would be a breakthrough of practical interest in this area of Analytical Chemistry, allowing to define proper estimates for the detection limits of the sensor.

The attempt to find the best calibration function was performed using the curve fitting software TableCurve2D [42]. Taking into account the prior knowledge of the general shape of the curve of the sensor response, the fitting was assessed by transition type functions. The TableCurve2D [42] built-in transition functions consist of a set of equations, that includes sigmoidal, Gaussian cumulative, Lorentzian cumulative, cumulative symmetric double sigmoidal, log normal cumulative, asymmetric sigmoidal, pulse cumulative, just to mention a few.

The calibration model that produces the most appropriate fit of the analytical response of the OF sensor is a cumulative symmetric double sigmoidal (SDS) function, with the highest $R^2$, $R^2_{aj}$ and $F$ values and the lowest standard error, in comparison to the other listed fifteen types of transition equations by TableCurve2D [42].

Fig. 4a shows the calibration model obtained for the entire range of the OF sensor response, including all repeated evaluations for the 9 amounts of toluene tested, in a total of 45 results. It can be seen that the fitting of the experimental points is perfectly appropriate and well described as a cumulative symmetric double sigmoidal (SDS) curve instead of a sigmoidal curve as initially foreseen. The same fitting was obtained for benzene and xylene cases.

Fig. 4b shows the residuals obtained for the SDS calibration model and allows to infer about the adequacy of the applied model, as the residual deviation varies between 1% and 5% and in only 2 cases, in a total of 45, reaches values higher than 5%, that is, −13% in one case (for determination of 0.02 μg of toluene) and +12% in another one (for determination of 0.03 μg of toluene).

The parameters of the SDS model calibration together with their statistics, obtained with TableCurve2D [42], are also shown in Table 1.

The results of the ANOVA confirm the argument that the fitting of the experimental results of calibration to a SDS model is a suitable approach, since the value of the *F*-test and its significance is very high ($p < 1 \times 10^{-6}$).

## 5. Estimative of the figures of merit of the OF sensors based on the SDS calibration model

### 5.1. Study of the properties of the SDS function as a calibration model

The study of the properties of the first and second derivatives of the SDS function was carried out in order to evaluate the possible applicability of this function as a calibration model for this type of sensors. It will show the variation of the sensor calibration sensitivity besides setting the lower and upper limits of the analytical system.

**Table 1**
Parameters and ANOVA obtained for both the linear and the SDS models used for the calibration of the OF sensor: DF—degrees of freedom, SS—sum of the squares, MS—mean squares, *F*—test *F*, *p*—probability.

| Linear calibration model | | | | | |
|---|---|---|---|---|---|
| Equation | Number of determinations | Correlation coefficient ($R$) | Determination coefficient ($R^2$) | Adjusted $R^2$ ($R^2_{aj}$) | Standard error |
| $y = -24.9 + 891x$ | 25 | 0.9997 | 0.9994 | 0.9994 | 0.326 |
| | Coefficients | Standard error | $t$ | $p$ | |
| Intercept | −24.9 | 0.3 | −87.5 | <0.0001 | |
| Slope | 891 | 5 | 193 | <0.0001 | |
| *ANOVA* | | | | | |
| | DF | SS | MS | F | $p$ |
| Regression | 1 | 3969.94 | 3969.94 | 37251.05 | < 0.0001 |
| Residual | 23 | 2.45 | 0.11 | | |
| Total | 24 | 3972.39 | 165.52 | | |
| Normality test | Passed ($p = 0.731$) | | | | |
| Constant variance test | Passed ($p = 0.925$) | | | | |

| SDS calibration model | | | | | |
|---|---|---|---|---|---|
| $R^2$ | 0.9992 | | | | |
| $R^2$aj | 0.9991 | | | | |
| Standard error | 0.5220 | | | | |
| $F$ | 12289.02 | | | | |
| Coefficient | Value | Standard error | $t$ | $p$ | |
| $A$ | 4.3123 | 0.1693 | 25.4744 | $< 1 \times 10^{-6}$ | |
| $B$ | 43.2568 | 0.2376 | 182.0782 | $< 1 \times 10^{-6}$ | |
| $C$ | 0.0571 | 0.0002 | 295.6867 | $< 1 \times 10^{-6}$ | |
| $D$ | 0.0486 | 0.0006 | 80.4716 | $< 1 \times 10^{-6}$ | |
| $E$ | $6.29 \times 10^{-4}$ | 0.0011 | 0.5531 | 0.5832 | |
| *ANOVA* | | | | | |
| | DF | SS | MS | $F$ | $p$ |
| Regression | 4 | 13394.38 | 3348.60 | 12289.02 | $<1 \times 10^{-6}$ |
| Residual | 40 | 10.90 | 0.27 | | |
| Total | 44 | 13405.28 | | | |

*5.1.1. First derivative of the SDS function*

Re-writing the SDS function obtained from TableCurve2D [42]: $y = A + B(2E(\ln(\exp((x + D/2)/E) + \exp(C/E))\ln(\exp((C + D/2)/E) + \exp(x/E))) + D)/(2D))$ under the following form:

$$y = \left(A + \frac{B}{2}\right) + \frac{BE}{D}\ln\left[e^{(x/E+D/2E)} + e^{C/E}\right] - \frac{BE}{D}\ln\left[e^{(C/E+D/2E)} + e^{x/E}\right] \quad (1a)$$

and defining new coefficients as follows:

$$A + \frac{B}{2} = a, \quad \frac{BE}{D} = b, \quad \frac{1}{E} = c, \quad \frac{D}{2E} = d, \quad \frac{C}{E} = f, \quad \frac{C}{E} + \frac{D}{2E} = f + d = g \quad (1b)$$

$$\text{it results :} \quad y = a + b\ln\left(e^{(cx+d)} + e^{f}\right) - b\ln\left(e^{g} + e^{cx}\right) \quad (1c)$$

which can be further simplified to: $y = a + b\ln(he^{cx} + i) - b\ln(j + e^{cx})$ where $e^d = h$, $e^f = i$, $e^g = j$

The first derivative $y'$ of the SDS function will then become:

$$y' = bc\left(\frac{1}{1 + ke^{-cx}} - \frac{1}{1 + je^{-cx}}\right) \quad (2a)$$

after taking

$$\frac{i}{h} = k \quad (2b)$$

The first derivative of the SDS function displays three notable regions: (a) a region where the slope is approximately zero for low values of $x$; (b) a region where the slope is almost constant and close to a value of about 900 for intermediate values of $x$; and (c) finally a region where the slope tends again to zero for higher values of $x$.

Setting the first derivative equal to zero in order to determine the existence of extremes:

$$y' = 0 \Leftrightarrow \frac{1}{1 + ke^{-cx}} - \frac{1}{1 + je^{-cx}} = 0 \Leftrightarrow ke^{-cx} = je^{-cx} \Leftrightarrow k = j \quad (3a)$$

There is no value of $x$ that effectively nullifies the first derivative.

$$\text{As} \quad k = \frac{i}{h} = e^{f-d} \quad \text{and} \quad j = e^{g} = e^{f+d}, \quad \text{then} \quad 1 + ke^{-cx} < 1 + je^{-cx} \quad (3b)$$

Therefore $y' > 0$ for all $x$, and consequently the SDS function is always increasing as $x$ increases, as it can be observed in Fig. 4.

*5.1.2. Second derivative of the SDS function*

The second derivative of the SDS function $y''$ shows the curvature of the function, and allows the evaluation of the inflexion points. By derivation of the first derivative of the SDS function:

$$y'' = bc\left(-\frac{-ke^{-cx}}{(1 + ke^{-cx})^2} + \frac{-je^{-cx}}{(1 + je^{-cx})^2}\right) \quad (4a)$$

That is,

$$y'' = bc^2e^{-cx}\left(\frac{k}{(1 + ke^{-cx})^2} - \frac{j}{(1 + je^{-cx})^2}\right) \quad (4b)$$

Equating (4b) to zero results,

$$x_I = \frac{f}{c}, \quad y_I = a \quad (5a)$$

or, in terms of the original parameters:

$$x_I = C, \quad y_I = A + \frac{B}{2} \quad (5b)$$

which are the coordinates of the inflexion point of the SDS function.

In fact:

$$y'' = 0 \Leftrightarrow \frac{k}{(1 + ke^{-cx})^2} - \frac{j}{(1 + je^{-cx})^2} = 0 \Leftrightarrow \sqrt{\frac{j}{k}} \times (1 + ke^{-cx}) = \pm(1 + je^{-cx}) \quad (5c)$$

thus,

$$\begin{cases} x_I = -\dfrac{1}{c}\ \ln\dfrac{1}{e^f} = -\dfrac{1}{c}(\ln 1 - \ln e^f) = \dfrac{f}{c} = \dfrac{C/E}{1/E} = C = 0.06 \\ x = -\dfrac{1}{c}\ \ln\left(\dfrac{-1}{e^f}\right) = \text{impossible in } \Re. \end{cases} \quad (5d)$$

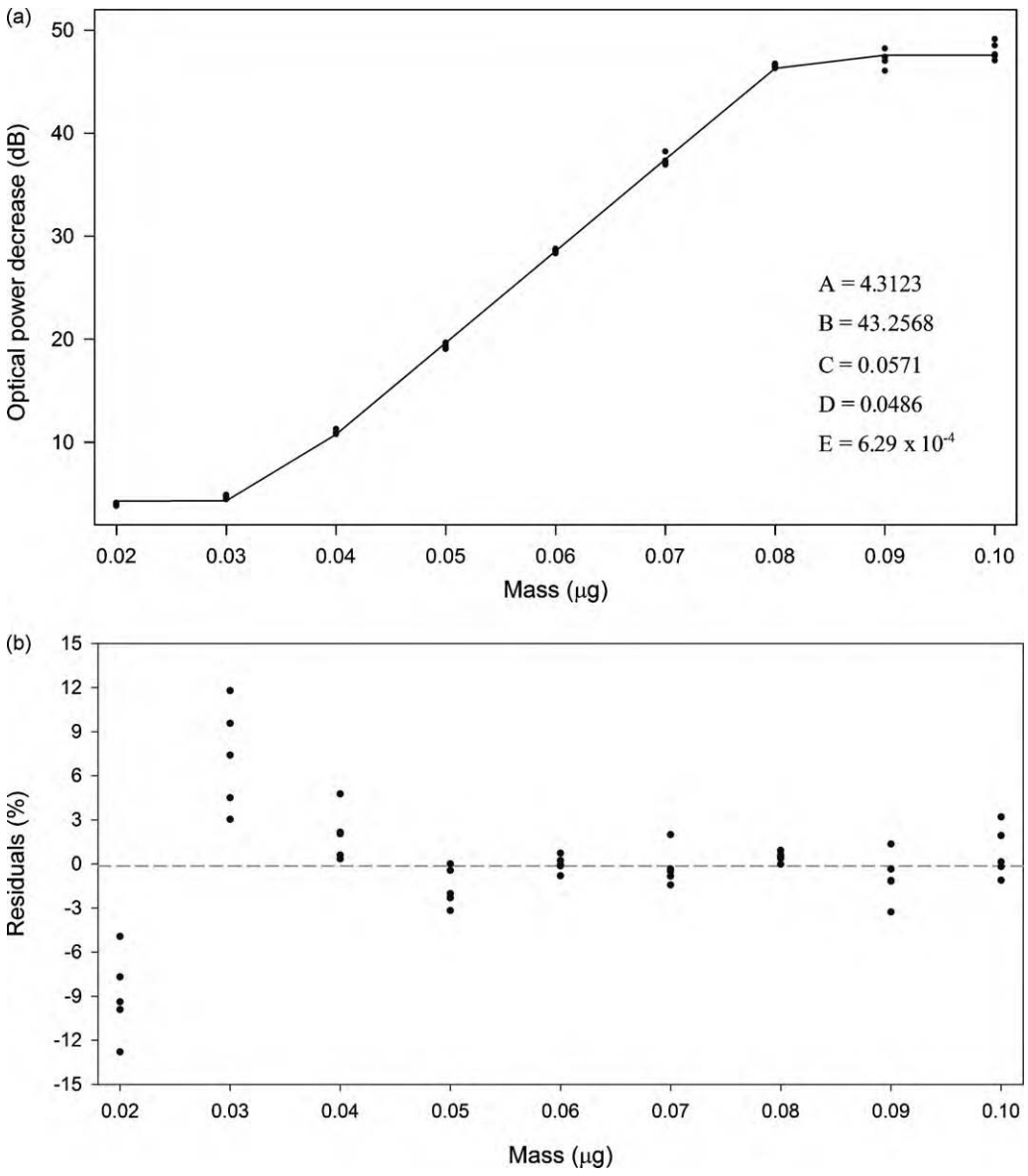


**Fig. 4.** Adjustment by SDS calibration model of the OF sensor response to the amounts of toluene tested (in a range between 0.02 and 0.10 μg) (a); residuals obtained for the SDS model (b).

The value of the SDS function at the inflexion point can be obtained by replacing $x_I = C$:

$$y(x_I) = (a + b\ \ln(he^{cx} + i) - b\ \ln(e^{cx} + j))_{(x=f/c=C)}$$
$$= a + b(\ln(e^{d+f} + e^{f}) - \ln(e^{f} + e^{f+d})) = a + b \times (0)$$
$$= a = A + \frac{B}{2} = 25.9 \quad (6a)$$

That is, the SDS function has an inflection point at $x_I = C = 0.06$ whose value is:

$$yI = A + \frac{B}{2} = 25.9 \quad (6b)$$

The second derivative, and thus the curvature, is always positive to the left of the inflexion point but only deviates significantly from zero at points very close to $x = 0.04$ μg. Symmetrically, the curvature is always negative to the right of the inflexion point, only deviating significantly from zero around $x = 0.08$ μg. This means that, between these two points, the particular SDS function obtained with the parameters of Table 1 is practically no distinguishable from to a straight line with positive slope; outside this region the SDS function is very nearly equal to its asymptotes.

*5.1.3. Approximating to a straight line*

The first derivative of the SDS function in the region between the above mentioned two points, which can be seen as defining the width of the transition, will enable the estimative of the linear equation included within the SDS calibration model, allowing also the calculation of the slope and therefore the determination of the calibration sensitivity.

The derivative gives the slope of $(x)$ at each point of $x$, which is the slope of the tangent at the indicated point:

$$y'(x_I) = bc\left(\frac{1}{1+ke^{-c(f/c)}} - \frac{1}{1+je^{-c(f/c)}}\right) = bc\frac{1-e^{-2d}}{1+e^{-2d}+2e^{-d}} \approx bc\frac{1-0}{1+0+0} \approx bc$$
$$y'\left(x_I = \frac{f}{c} = C\right) \approx bc \approx \frac{BE}{D} \times \frac{1}{E} \approx \frac{B}{D} \quad (7)$$
$$y'(x_I) \approx 890$$

Thus, it is possible to infer that in the zone of constant non-zero slope observed for the first derivative of the SDS function, a value of 890 can be established. Such is almost the same value

of the slope in the linear model used for calibration as shown in Fig. 3b.

### 5.2. Calibration sensitivity of the OF sensors based on the SDS model

After the determination of $x_I$ ($x_I = C$) and $y_I$ ($y_I = A + B/2$) the expression of the equation of the tangent line at the inflection point can be determined defining $t$ as:

$$t = \frac{1 - e^{-2d}}{1 + e^{-2d} + 2e^{-d}} \tag{8}$$

and resulting

$$y - y_I = m(x - x_I) \Leftrightarrow y = \left(A + \frac{B}{2} - \frac{BC}{D}t\right) + \left(\frac{B}{D}t\right)x \tag{9}$$

Replacing the constants $A$, $B$, $C$, $D$ and $E$ by their particular values in this study case, $t$ becomes very close to 1 and the equation for the tangent can be written as:

$$y = -24.9 + 890x \tag{10}$$

The sensitivity of the OF sensor obtained by the SDS calibration model (890 dB $\mu g^{-1}$) is almost the same value as calculated from the linear model ($y = -24.9 + 891x$) to the linear response range of the OF sensor. This conclusion suggests that although more complex, the SDS function is a general calibration model with a linear region and applicable to the full working range of the determinant.

### 5.3. Detection limits of the OF sensors based on the SDS model

A typical response of an OF sensor to volatile organic compound could be characterized by three analytical regions. The first one is referent to the sensor behavior for lower amounts of analyte, in which no significant changes in signal occurs. In the second region, a rapid change in signal occurs over a narrow range of analyte amounts. Finally, the third region reflects the sensor behavior for higher analyte amounts, at which the system reaches a maximum plateau in terms of its detection capability and an almost constant signal could be observed for increasing values of analyte.

This sensor behavior and regarding the estimative of the capabilities of analytical system, implies the establishment of both a lower detection limit and an upper detection limit.

For the calculation of the lower detection limit several different approaches can be considered. Firstly, and considering the linear behavior of the sensor, the estimate of the detection limit obtained for the OF sensor was found to be 1.1 ng taking into account the classical criterion based on 3 times the residual standard deviation [43]. However, replacing the $x$ value of 1.1 ng (0.0011 μg) in the linear equation an optical power variation of −23.9 dB is obtained, which represents an increase of power of about 24 dB, with no physical meaning in the case of the developed sensor. This calculated positive value of optical power variation, is due to the fact that the sensor does not follow an analytical linear response for amounts much less than 0.04 μg (lowest amount of the calibration curve) as assumed in the linear model.

In this case, the classical criterion for calculation of the detection limit based on $y_{DL} = y_B + 3s_B$ [43] is not appropriate for assessing the detection limit of the OF sensor. This figure of merit must be redefined in the case of the OF sensor, when the response is not linear, in order to have physical meaning and any use in analytical terms.

A second approach for the calculation of the lower detection limit could be based on the 95% confidence interval of the first point of the calibration curve using $x_0 \pm ts_{x_0}$, $(n-2)$ [43] degrees of freedom, where $s_{x_0}$ is given by,

$$s_{x_0} = \frac{s_{y/x}}{b}\left\{1 + \frac{1}{n} + \frac{(y_0 - \bar{y})^2}{b^2 \sum_i (x_i - \bar{x})^2}\right\}^{1/2} \tag{11}$$

Using this criterion and considering the linear behavior of the OF sensor, the detection limit was found to be 40.3 ± 0.9 ng.

A more exactly determination of the detection limits, both the lower and upper detection limit, can be performed by using the SDS calibration model. Since OF sensors are often characterized by a limited dynamic range of analyte measurement, the estimative of the upper detection limit becomes a useful tool regarding the evaluation of the analytical performance of the OF sensor.

The interception of the tangent of the inflection point with the horizontal asymptotes, allows determining the lower limit of detection ($x_m$) and the upper limit of detection ($x_M$) of the SDS calibration model.

A line with the equation $y = U$ is a horizontal asymptote of the function, if any of the limits $\lim_{x \to \pm\infty} f(x) = U$ is observed. Determining the limit of the SDS function when $x$ approaches $+\infty$, gives:

$$\begin{aligned} &\lim_{x \to +\infty} y = a + bd = \left(A + \frac{B}{2}\right) + \left(\frac{BE}{D}\right)\left(\frac{D}{2E}\right) = A + B \\ &\lim_{x \to +\infty} y = 47.6 \end{aligned} \tag{12}$$

The horizontal asymptote to the left has a value of 47.6 dB.

Determining the limit of the SDS function when $x$ approaches $-\infty$, gives:

$$\begin{aligned} &\lim_{x \to -\infty} y = \lim_{x \to -\infty} (F + G\ \ln(Ne^{Hx} + P) - G\ \ln(e^{Hx} + Q)) = F - GH = A \\ &\lim_{x \to -\infty} y = 4.31 \end{aligned} \tag{13}$$

The horizontal asymptote to the right has a value of 4.31 dB.

Intersecting the tangent at the inflection point with the two asymptotes of the function, an approximate value of the points $x_m$ (minimum or lower) and $x_M$ (maximum or upper) can be determined.

The interception of the tangent at the inflection point with the asymptotes of the function gives the points: $x_m = C - D/2t$ and $x_M = C + D/2t$, which define the function's width as follows:

$$x_M - x_m = \frac{D}{t} \tag{14}$$

Since $t = (1 - e^{-2d})/(1 + e^{-2d} + 2e^{-d})$ and $d = D/2E$, it can be seen that when $d \to \infty$ then $t \to 1$. Therefore the width of the function approaches $D$, and the tangent of the inflection point approaches:

$$y = \left(A + \frac{B}{2} - \frac{BC}{D}\right) + \left(\frac{B}{D}\right)x \tag{15}$$

(i) Calculation of the lower limit of the sensor

Intercepting the tangent at the inflection point, with the horizontal asymptote $y = A$, gives:

$$A = \left(A + \frac{B}{2} - \frac{BC}{D}\right) + \left(\frac{B}{D}\right)x \Leftrightarrow x_m = C - \frac{D}{2} = 0.033 \tag{16a}$$

Therefore the lower detection limit ($x_m$) obtained for the sensor with the SDS model is 0.033 μg.

(ii) Calculation of upper limit of the sensor

Intercepting the tangent at the inflection point, with the asymptote $y = A + B$, gives:

$$A + B = \left(A + \frac{B}{2} - \frac{BC}{D}\right) + \left(\frac{B}{D}\right)x \Leftrightarrow x_M = C + \frac{D}{2} = 0.081 \tag{16b}$$

Therefore the upper limit ($x_M$) obtained for the sensor with the SDS model is 0.081 μg.

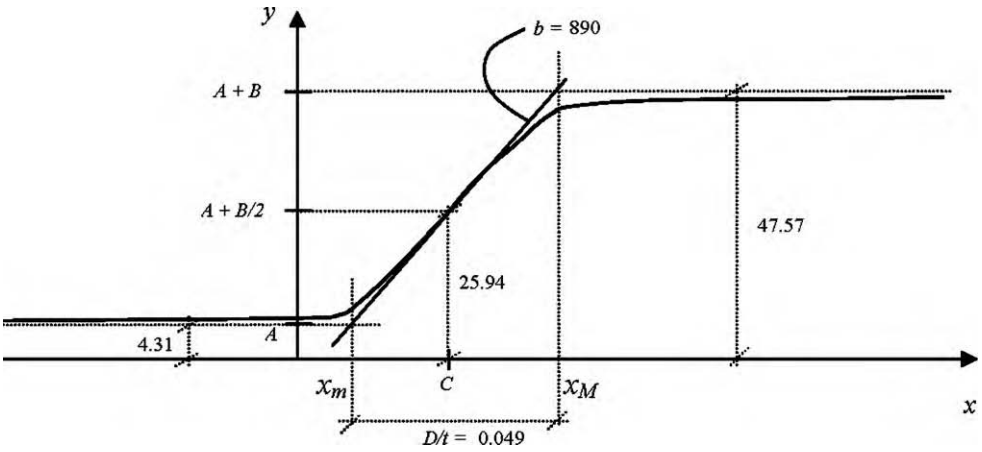


**Fig. 5.** Schematic representation of the tangent at the inflection point, the horizontal asymptotes of the SDS function and the lower and the upper detection limits.

Fig. 5 summarizes and shows a schematic representation of the tangent at the inflection point, the horizontal asymptotes of the SDS function and the lower and the upper detection limits.

## 6. Analytical advantages of the SDS calibration model in relation to linear model

The SDS calibration model includes not only the analytical linear response of the sensor defined by the equation $y = -24.9 + 890x$, but also considers the response of the OF sensor beyond the lower and upper limit of this linear zone. The linear calibration model restricts the analysis of the analytical response of the OF sensor to the linear response zone. In the past [6–10], the use of a linear model for the estimative of the figures of merit of the sensor, namely the detection limit, caused some problems in terms of their analytical usefulness. Thus, the SDS calibration model constitutes an adequate alternative to the linear calibration model, since it includes the full working range of the target analyte, also describing accurately the sensor performance through the appropriate estimative of its figures of merit.

## 7. Conclusions

A cumulative symmetric double sigmoidal (SDS) function has been proposed as a general model for describing the analytical response of an OF sensor. The SDS model includes a linear calibration zone for which is possible to calculate the sensitivity of the method (890 dB $\mu g^{-1}$), established between a lower (0.033 $\mu g$) and an upper detection limit (0.081 $\mu g$) of the analytical system. This calibration model was shown to be valid for the whole entire range of the analytical response of the OF sensor and compares more advantageously with a linear model, since it provides estimatives of the figures of merit of the sensor system with analytical interest and statistical significance.

## Acknowledgements

This work has been developed under the scope of the FCT (Portugal) funded research projects PTDC/QUI/70970/2006 and FCOMP-01-0124-FEDER-010896: "Development of a new Optical Fiber Biosensor for Determination of Catecholamines (CATSENSOR)" and POCTI/CTA/44899/02: "Development of a new Optical Fiber Chemical Sensor for in situ monitoring of VOCs (VOCSENSOR)". A Ph.D. Grant (SFRH/BD/17288/2004) awarded to Lurdes I.B. Silva is also gratefully acknowledged.

## References

[1] O.S. Wolfbeis, Anal. Chem. 80 (2008) 4269–4283.
[2] C. Elosua, I.R. Matias, C. Bariain, F.J. Arregui, Sensors 6 (2006) 1440–1465.
[3] B. Kuswandi, R. Andres, R. Narayanaswamy, Analyst 126 (2001) 1469–1491.
[4] L.I.B. Silva, F.D.P. Ferreira, A.C. Freitas, T.A.P. Rocha-Santos, A.C. Duarte, Talanta 80 (2009) 853–857.
[5] M.N. Taib, R. Narayanaswamy, Analyst 120 (1995) 1617–1625.
[6] L.I.B. Silva, T.A.P. Rocha-Santos, A.C. Duarte, Talanta 78 (2009) 548–552.
[7] L.I.B. Silva, A.M. Costa, A.C. Freitas, T.A.P. Rocha-Santos, A.C. Duarte, Int. J. Environ. Anal. Chem. 89 (2009) 183–197.
[8] L.I.B. Silva, T.A.P. Rocha-Santos, A.C. Duarte, Global Nest J. 10 (2008) 217–225.
[9] L.I.B. Silva, T.A.P. Rocha-Santos, A.C. Duarte, Sens. Actuator B 132 (2008) 280–289.
[10] L.I.B. Silva, A.V. Panteleitchouk, A.C. Freitas, T.A.P. Rocha-Santos, A.C. Duarte, Anal. Methods 1 (2009) 100–107.
[11] Y. Ueno, T. Horiuchi, O. Niwa, H.-S. Zhou, T. Yamada, I. Honma, Sens. Actuator B 95 (2003) 282–286.
[12] F. Abdelmalek, J.M. Chovelon, M. Lacroix, N. Jaffrezic-Renault, V. Matejec, Sens. Actuator B 56 (1999) 234–242.
[13] A. Abdelghani, N. Jaffrezic-Renault, Sens. Actuator B 74 (2001) 117–123.
[14] S.-F. Cheng, L.-K. Chau, Anal. Chem. 75 (2003) 16–21.
[15] C. Elosua, C. Bariain, I.R. Matias, A. Rodriguez, E. Colacio, A. Salinas-Castillo, A. Segura-Carretero, A. Fernandez-Gutiérrez, Sensors 8 (2008) 847–859.
[16] C. Elosua, I.R. Matias, C. Bariain, F.J. Arregui, Sensors 6 (2006) 578–592.
[17] C. Bariain, I.R. Matías, I. Romeo, J. Garrido, M. Laguna, Sens. Actuator B 76 (2001) 25–31.
[18] C Bariain, I.R. Matias, C. Fdez-Valdivielso, C. Elosua, A. Luquin, J. Garrido, M. Laguna, Sens. Actuator B 108 (2005) 535–541.
[19] C. Elosua, C. Bariain, I.R. Matías, F.J. Arregui, A. Luquin, M. Laguna, Sens. Actuator B 115 (2006) 444–449.
[20] C Elosua, C. Bariain, I.R. Matías, F.J. Arregui, A. Luquin, E. Vergara, M. Laguna, Sens. Actuator B 130 (2008) 158–163.
[21] C. Elosua, C. Bariain, I.R. Matias, F.J. Arregui, E. Vergara, M. Laguna, Sens. Actuator B 137 (2009) 139–146.
[22] R Narayanaswamy, Analyst 118 (1993) 317–322.
[23] P. Hua, J.P. Hole, J.S. Wilkinson, G. Proll, J. Tschmelak, G. Gauglitz, M.A. Jackson, R. Nudd, H.M.T. Griffith, R.A. Abuknesha, J. Kaiser, P. Kraemmer, Opt. Express 13 (2005) 1124–1130.
[24] V.S. Thompson, C.M. Maragos, J. Agric. Food Chem. 44 (1996) 1041–1046.
[25] F.B.M. Suah, M. Ahmad, M.N. Taib, Sens. Actuator B 90 (2003) 182–188.
[26] T.E. Brook, M.N. Taib, R. Narayanaswamy, Sens. Actuator B 38–39 (1997) 272–276.
[27] M.N. Taib, R. Andres, R. Narayanaswamy, Anal. Chim. Acta 330 (1996) 31–40.
[28] F.B.M. Suah, M. Ahmad, M.N. Taib, Sens. Actuator B 90 (2003) 175–181.
[29] D. King, W.B. Lyons, C. Flanagan, E.J. Lewis, Opt. A: Pure Appl. Opt. 5 (2003) 69–75.
[30] M.N. Taib, R. Narayanaswamy, Sens. Actuator B 38–39 (1997) 365–370.
[31] J.M. Sutter, P.C. Jurs, Anal. Chem. 69 (1997) 856–862.
[32] K.S. Johnston, K.S. Booksh, T.M. Chinowsky, S.S. Yee, Sens. Actuator B 54 (1999) 80–88.
[33] J.-P. Conzen, J. Biirck, H.-J. Ache, Fresenius J. Anal. Chem. 348 (1994) 501–505.
[34] K.S. Johnston, S.S. Yee, K.S. Booksh, Anal. Chem. 69 (1997) 1844–1851.

[35] Y.-F. Chang, R.-C. Chen, Y.-J. Lee, S.-C. Chao, L.-C. Su, Y.-C. Li, C. Chou, Biosens. Bioelectron. 24 (2009) 1610–1614.
[36] Z. Jin, Y. Su, Y. Duan, Sens. Actuator B 72 (2001) 75–79.
[37] A.S. Kocincova, S.M. Borisov, C. Krause, O.S. Wolfbeis, Anal. Chem. 79 (2007) 8486–8493.
[38] J.C. Solís, E. De la Rosa, E.P. Cabrera, Fiber Integr. Opt. 26 (2007) 335–342.
[39] L.F. Capitán-Vallvey, E. Arroyo-Guerrero, M.D. Fernández-Ramos, L. Cuadros-Rodríguez, Anal. Chim. Acta 561 (2006) 156–163.
[40] F.L. Ribeiro, M.C. Ferreira, S.C. Morano, L.R. Silva, R.P. Schneider, Quim. Nova 31 (2008) 164–171.
[41] J.N. Miller, Analyst 116 (1991) 3–14.
[42] TableCurve2D (Curve Fitting Software), Jandel Scientific, Erkrath, Germany, 1996.
[43] J.N. Miller, J.C. Miller, Statistics and Chemometrics for Analytical Chemistry, fifth ed., Pearson Prentice Hall, New York, 2005.